

Capture of negative muons in atoms*

P. K. Haff, P. Vogel, and A. Winther†

California Institute of Technology, Pasadena, California 91109

(Received 15 April 1974)

The frictional force derived from the stopping power of an electron gas is used in the classical equation of motion for the negative muons. We calculate the energy spectrum of the captured muons and the angular momentum distribution of muons at the energy of the electronic K orbit. The resulting $P(l)$ distribution closely resembles the statistical $2l + 1$ distribution.

As was stressed by Fermi and Teller in 1947,¹ the capture of a negative muon in an atom may well be treated in terms of classical physics. A muon moving through an atom experiences a gradual loss of energy and angular momentum due to collisions with the electrons, and the effect of these collisions on the muon can be described by introducing a frictional force in the classical equations of motion. This picture breaks down when the muon has lost so much energy that it moves in the region of the electronic K shell, where the Auger transitions that give rise to the frictional force should be treated quantum mechanically.

Several workers have used this prescription to study the capture of negative heavy particles. The most recent calculations have been made by Leon and Seki.² The present note follows the general lines of their work, but differs in the conclusions mainly because it includes the crucial interrelation between stopping and capture.

The initial slowing down of a muon to velocities of the order of $v \approx v_0 Z^{1/2}$ (with $v_0 = e^2/\hbar$ and Z being the charge number of the atom) proceeds according to standard stopping theory. For lower meson velocities, distant collisions do not contribute to the energy loss, and the stopping is mainly a function of the local electron density $\rho(\vec{r})$. According to Lindhard,³ the stopping power in this region of velocities and for not too large impact parameters can be described by the frictional force

$$\vec{F} = -\frac{\vec{v}}{v} \frac{dE}{dx} = -\frac{4m^2 e^4}{3\pi\hbar^3} C_1(\chi) \vec{v}, \quad (1)$$

where m is the electron mass and \vec{v} is the muon velocity. The function $C_1(\chi)$ can be estimated from the stopping power of a free-electron gas⁴ as

$$C_1(\chi) = \frac{1}{2(1+\chi^2/3)^2} \left[\ln \left(\frac{1+\frac{2}{3}\chi^2}{\chi^2} \right) - \frac{1-\frac{1}{3}\chi^2}{1+\frac{2}{3}\chi^2} \right]. \quad (2)$$

It is a slowly varying function of the electron den-

sity $\rho(r)$ through

$$\chi^2 = (me^2/\hbar^2)[3\pi^5\rho(\vec{r})]^{-1/3}, \quad (3)$$

as given in Ref. 4.

In the numerical calculations we have used the Lenz-Jensen model⁵ for the electron density and for the average potential $U(r)$ of the muon in the atom. The effect of radiation is rather insignificant. In our calculation it was included approximately by using the force

$$\vec{F}_{\text{rad}} = -\frac{2}{3} \frac{e^2}{m_\mu c^3} \frac{d}{dt} \vec{v} U(r). \quad (4)$$

Introducing the forces (2) and (4) in the classical equations of motion one may follow the trajectory of the muon through the atom. For a given impact parameter and initial energy the muon may either leave the atom with a loss of energy ΔE or it may be captured. The energy loss for $Z=55$ is illustrated in Fig. 1 as a function of the square of the impact parameter b^2 for different initial energies E . The points where these curves reach the values $\Delta E = E$ indicate the limits of the intervals in b^2 where capture will take place.

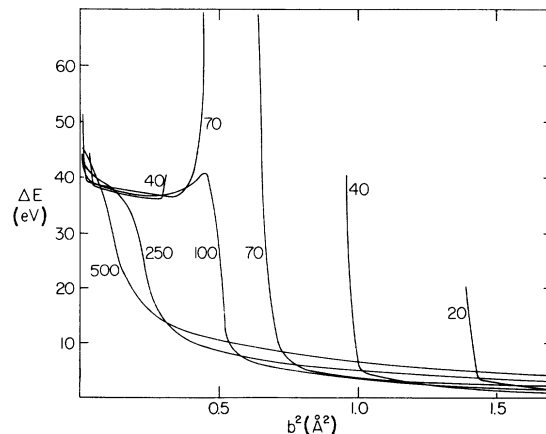


FIG. 1. Energy loss ΔE for $Z=55$ as a function of the squared impact parameters in angstroms squared. Each curve is labeled by the energy of the incoming muon in eV.

From these curves one may in principle calculate the energy distribution of the captured muons, but the problem is nontrivial, leading to equations of the type discussed in Ref. 6. We have instead used a Monte Carlo calculation where the fate of a muon with an initial energy of 250–500 eV was followed from collision to collision until it was captured. The trajectories for the captured muons were followed until they reached a binding energy where quantal effects become important for the further transitions to the muonic ground state. The transition between this third stage of the capture process and the classical region was studied by comparing existing quantum mechanical Auger-cascade calculations with the classical rate of energy and angular momentum loss, and it was found that they agree rather well when the principal quantum number of the muon is $n \approx 13$ –14. Thus the classical trajectories were followed until this region was reached, i.e., until the total energy was $E = -Z^2 R_\infty$. The angular momentum was then recorded.

The resulting distribution $P(L)$ of angular momenta L is illustrated in Fig. 2 for $Z=55$. Trans-

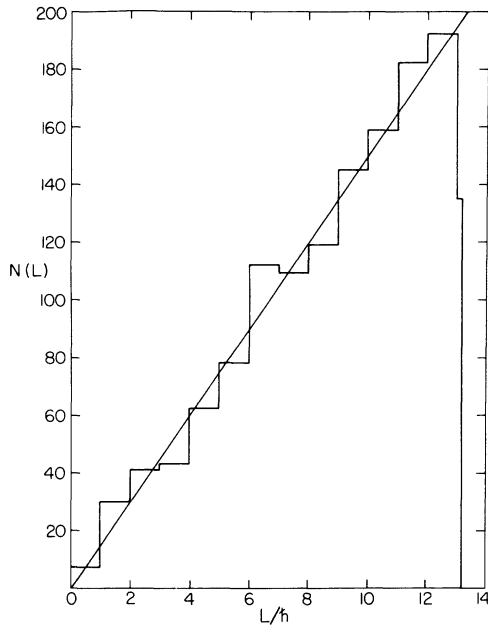


FIG. 2. Histogram of the $N(L)$ distribution for $Z=55$ obtained by a Monte Carlo calculation with 1306 samples. The last bin is squeezed because the maximum classical angular momentum equals $13.2\hbar$ at the cutoff energy $E = -Z^2 R_\infty = -41140$ eV.

lating L into the quantum number l by $L \rightarrow (l + \frac{1}{2})\hbar$, it is seen that the distribution follows the rule $P(l) \sim (2l+1)e^{\alpha l}$ with $\alpha = 0.001(8)$ in agreement with experiments on muonic x rays.⁷ A similar $P(l)$ distribution was calculated for $Z=19$ with the result $\alpha = 0.045(11)$. The $P(l)$ distributions obtained with the initial energies 250 or 500 eV are statistically indistinguishable.

The disagreement between these results and those of Ref. 2 is mainly due to the assumption in Ref. 2 of a flat energy distribution of the captured particles. In our case no *a priori* assumption about the energy distribution is made. Instead, it is calculated using the same mechanism for both the capture and slowing down processes. This is a crucial step; we were able to reproduce in a qualitative way the angular-momentum distribution function $P(l)$ of Ref. 2 when we made the assumption that the mesons are captured with the same probability at all energies.

In our calculations the muons are predominantly captured at energies near the plateau of Fig. 1. Figure 3 shows the calculated energy distribution of the captured muons; a similar histogram for $Z=19$ has a maximum at 15–20 eV.

We plan to use the above described method for the more complicated cases of the capture of negative particles (muons, pions, kaons, etc.) in mixtures, crystals, and molecules.

We thank Professor T. Tombrello for many interesting discussions.

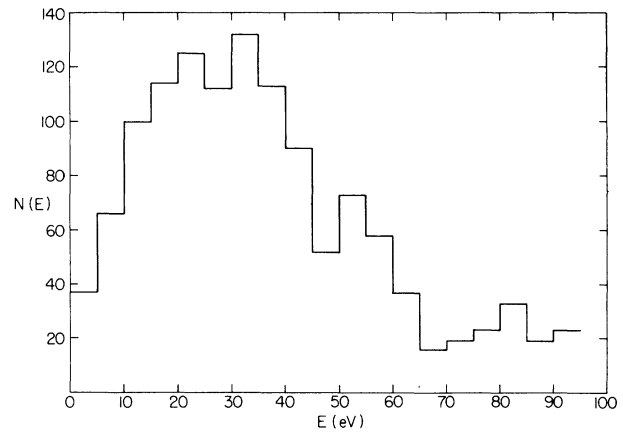


FIG. 3. Histogram of the muon energy distribution $N(E)$ for $Z=55$ obtained by a Monte Carlo calculation with 1306 samples. Of the samples 57 were captured above 95 eV and are not included in the figure.

*Work supported jointly by the National Science Foundation [GP-28027] and the U. S. Atomic Energy Commission AEC AT[04-3]-63.

†Permanent address: Niels Bohr Institute, DK-2100, Copenhagen, Denmark.

¹E. Fermi and E. Teller, Phys. Rev. 72, 399 (1947).

²M. Leon and R. Seki, Phys. Rev. Lett. 32, 132 (1974).

³J. Lindhard, Mat. Fys. Medd. Dan. Vid. Selsk. 34, No. 14 (1965).

⁴J. Lindhard and A. Winther, Mat. Fys. Medd. Dan. Vid. Selsk. 34, No. 4 (1964).

⁵The Lenz-Jensen model is an analytic version of the statistical Thomas-Fermi atomic model. For details see P. Gombás: *Die Statistische Theorie des Atoms* (Springer Verlag, Vienna, 1949).

⁶J. Lindhard, V. Nielsen, M. Scharff, and P. V. Thomsen, Mat. Fys. Medd. Dan. Vid. Selsk. 33, No. 10 (1963).

⁷For a discussion of the experimental evidence about the $P(l)$ distribution see, for example, H. Backe *et al.* Nucl. Phys. A 189, 472 (1972).